The solar interior

H. M. Antia

Tata Institute of Fundamental Research, Homi Bhabha Road, Mumbai 400 005, India

The Sun being the nearest star, provides us a unique opportunity to study stellar processes in sufficient detail to test theories of stellar structure and evolution. Although the solar interior is not directly accessible to observations, development of helioseismology during the last three decades has enabled us to study the structure and dynamics of solar interior with unprecedented accuracy. Some of these developments are described in this article.

Keywords: Helioseismology, neutrino fluxes, solar interior, standard solar model.

Introduction

THE Sun provides the energy to sustain life and to drive the climate and weather on the Earth and hence has been observed since time immemorial. The first scientific measurement related to Sun was probably the measurement of its angular diameter by Archimedes in the third century BC. He measured the solar diameter to be between 1/200 and 1/164 of a right angle or 27′–32′56″, which agrees with the current estimate. Archimedes probably did not know the distance to the Sun and hence was not able to measure the actual solar diameter. First detailed scientific observation of the Sun was probably undertaken by Galileo in 1609 when he used a telescope to observe the Sun. His painstaking study of sunspots led to the conclusion that the Sun is rotating and he was able to measure the rotation period of the Sun. The study of planetary orbits in the solar system led to Newton's theory of gravity. During the last century, again the orbit of planet mercury provided one of the early tests of the general theory of relativity. Apart from theory of gravitation, helium which is the second most abundant element in the universe was discovered in the solar prominence spectrum. Thus, the Sun has played a central role in development of physics.

During the last few centuries, a detailed observation of the Sun over the entire range of electromagnetic spectrum from radio to γ-rays has yielded valuable information about the solar surface and overlying layers. These observations along with the development in physics enabled us to understand the basic picture of Sun and other stars. The stars are now believed to be nearly spherical self-gravitating mass of plasma, which sustains the energy through thermonuclear reactions near the centre. The energy released in the core diffuses outwards through radiation or convection, until it reaches the surface, which is known as the photosphere. Since the Sun doesn't have a well-defined boundary, the definition of surface is somewhat ambiguous, but it is roughly the layer above which the atmosphere is optically thin and hence the energy is radiated out into the surrounding space. Contrary to expectation, the temperature in the solar atmosphere reaches a minimum value about 500 km above the photosphere and beyond that it increases rapidly to a few million degrees K in the corona. These regions in the solar atmosphere are controlled by the magnetic field, which was first detected in the sunspots by Hale[1] soon after the discovery of the Zeeman effect. While a number of interesting energetic phenomenon occur in the solar atmosphere, in this article I would only consider the solar interior.

The solar photosphere and the overlying layers are the regions where spectral lines are formed and hence these layers can be studied spectroscopically. On the other hand, layers below the photosphere are not directly accessible to observations and until recently all information about the solar interior was based only on the so-called solar models, which are basically solutions of equations of stellar structure. These equations are based on known laws of physics with some simplifying assumptions and the resulting stellar models need to be tested independently. Historically, the first direct test of solar models was attempted through detection of neutrinos produced in nuclear reactions in the solar core[2]. Since neutrinos are weakly interacting, they are expected to pass through the Sun and in principle, should be observable at the Earth. However, the observed flux of solar neutrinos was found to be about a factor of 3 lower than what was expected from the solar model, thus raising questions about validity of solar models. As a result, a considerable effort was made to improve the solar models by including various processes, like rotation, magnetic field, mixing of material in solar core, etc. which are not included in conventional solar models. Apart from new processes, the standard physical treatment of solar material was also improved considerably, but none of these efforts led to an acceptable solar model with observed neutrino flux. Around the same time, an independent probe of solar structure based on study of solar oscillations became available. This study has been referred to as helioseismology, in analogy with the seismic study of the

e-mail: antia@tifr.res.in

Earth's interior. Unlike the Earth, where seismic waves are triggered by a seismic event, like an earthquake, in the Sun these waves are continuously produced by turbulent convection near the surface[3]. The observed oscillations are superposition of about a million independent modes of solar oscillations, each with an amplitude of less than a metre per second. Like any musical instrument the Sun oscillates in a set of well-defined modes with frequencies determined by internal structure and dynamics. Helioseismology allows us to study the solar interior in much more detailed manner than the neutrino fluxes and it turned out that the standard solar model with some improvements in input physics agreed well with seismic constraints. With these developments it became clear that the discrepancy in the solar neutrino flux is not due to solar model and subsequently, it has been confirmed that this is because the neutrinos oscillate from one flavour to another during the course of their travel from solar core to the Earth[4]. Thus, the study of the Sun provided a laboratory for testing physics beyond the standard model of particle physics.

The global characteristics of the Sun are now measured to a reasonable accuracy. The standard value of solar radius $R_\odot = (6.9599 \pm 0.0007) \times 10^{10}$ cm (ref. 5), refers to the observed edge of the photosphere. This may not be the same as the radius used in a solar model, where the surface is defined as the layer where optical depth measured from outside is of order of unity. The observed surface may be about 500 km above that in a solar model[6]. This difference can only be estimated by a detailed atmospheric model including radiative transfer and is somewhat uncertain. An alternative is to calibrate the model radius using frequencies of f-modes, which give a value 200–300 km smaller than the standard value[7,8]. The total luminosity has been estimated to be 3.842×10^{33} erg s^{-1}. The solar mass is estimated to be 1.989×10^{33} g and the main uncertainty in this estimate comes from errors in the universal gravitational constant, G. The product $GM_\odot$ is known very accurately from planetary orbits and any variation in value of solar mass must be compensated by an opposite variation in the gravitational constant[9].

The standard solar model

The standard solar model is the solution of the equations of stellar structure and evolution as applicable to the Sun. These equations are obtained by assuming that the Sun is spherically symmetric and in hydrostatic and thermal equilibrium. Further, it is assumed that the Sun was chemically homogeneous at the time of its formation. It is not clear if these assumptions are valid. For example, the Sun is known to be rotating and has magnetic field which give rise to departures from spherical symmetry, but these are known to be less than a part in 10^5. Thus to a good approximation, the Sun can be assumed to be spherically symmetric. Similarly, the Sun is not static as we can see motions in the convection zone near the solar surface, but after suitable averaging the velocity is expected to vanish. The mechanical time-scale, which is given by the sound travel time across the Sun is of the order of an hour and one would expect the Sun to have reached mechanical equilibrium over its life of 4.57 billion years. The assumption of thermal equilibrium essentially implies that the energy generated in the solar core is emitted from the surface, even though it would take several million years to diffuse from the centre to the surface. This implies that the Sun is in a steady state. The solar radius and luminosity change on the evolutionary time-scale of billion years. Thus, the solar evolutionary calculations show that luminosity has increased by about 30% during its life-time.

Apart from these assumptions any solar model must satisfy the global constraints, like the solar mass, radius, luminosity and age. The chemical composition of the solar material can in principle, be determined from spectroscopy. However, this gives only the surface composition and further some important elements, like the noble gases do not form lines at the photosphere and hence their composition is more uncertain as it has to be determined from coronal lines where the physics is more uncertain. Traditionally, astronomers denote the composition by three numbers X, Y, Z, which respectively, give the mass fraction of hydrogen, helium and the rest of elements, with $X + Y + Z = 1$. The surface abundances mainly provide us the ratio X/Z as the helium abundance is rather difficult to determine spectroscopically, although helium was discovered in the solar spectrum by Janssen and Lockyer. Janssen observed some unknown line in spectra from solar prominence during and after the total solar eclipse on 18 August 1868 from Guntoor, India. These lines were later identified to be from helium. The chemical composition in the Sun primarily changes due to nuclear reactions, which effectively converts hydrogen to helium in the core. Apart from this there is a slow diffusion of helium and heavy elements towards the centre. Although the time-scale for diffusion is larger than the solar age, a small fraction of these elements have diffused inwards and hence the surface composition does not reflect the initial composition of the Sun. The outer 30% of the solar radius is believed to be the convection zone, where energy is primarily transmitted by convective motions. These convective eddies also mix the material and hence, the composition of the outer part of the Sun is believed to be homogeneous.

The equations of stellar structure can be written as (e.g. Cox and Giuli[10]):

$$\frac{dP(r)}{dr} = -\frac{Gm(r)}{r^2}\rho(r), \tag{1}$$

$$\frac{dm(r)}{dr} = 4\pi r^2 \rho(r), \tag{2}$$

$$\frac{dL(r)}{dr} = 4\pi r^2 \rho(r)\varepsilon, \quad (3)$$

$$\frac{L(r)}{4\pi r^2} = -\frac{16\sigma T^3}{3\kappa\rho}\frac{dT}{dr}, \quad (4)$$

where P is the pressure, ρ the density, T the temperature, σ the Stefan's constant, G the gravitational constant, $m(r)$ the mass enclosed in spherical shell of radius r, $L(r)$ is the total energy generated within the radius r. Here ε is the rate of nuclear energy production per unit mass and κ the opacity. Both these quantities can be estimated from the known nuclear and atomic physics. Apart from these we also need an equation of state to relate P, ρ, T and composition. Equation (4) is valid only in the radiative region as it only includes the transport of energy by radiation. As the temperature decreases with increasing radius, the opacity increases and at some stage the opacity is too large to allow transmission of all energy through radiation. At this stage, which in the present Sun occurs around $r = 0.713R_\odot$, convection takes over and the region is known as the convection zone. There is no rigorous theory to calculate the convective flux in the convection zone and stellar structure calculations typically use the so-called mixing-length theory (e.g. Cox and Giuli[10]). This is not a serious limitation, as in most of the convection zones, the density is fairly large and convection is very efficient in transmitting energy. In such conditions, the temperature gradient is very close to the adiabatic value, which is the minimum required for convection to take place. However, in the outermost layers near the surface, the density is rather low ($\approx 10^{-6}$ g cm^{-3}) and temperature gradient can become significantly superadiabatic. In this region, the treatment of convection is important and this is a major source of uncertainty in stellar models. The effect of this uncertainty is minimized by introducing an adjustable parameter, α in the mixing length theory, which in some sense calibrates the entropy in the convection zone and determines the structure of the lower part of the convection zone.

In order to solve these equations, we also need appropriate boundary conditions. At the centre, $r = 0$ we have $m(r) = 0$ and $L(r) = 0$ as the natural boundary conditions. At the surface, the density and pressure should tend to zero as the temperature approaches the surface value. These equations along with the boundary conditions can be solved if the composition of solar material is known. Initially, we start the solar evolution calculations with a uniform composition and the composition gradient is built up through nuclear reactions in the core and slow diffusion of helium and heavy elements in the radiative interior. As the composition changes, the Sun evolves from its zero age main sequence configuration to its present state at an age of about 4.57×10^9 yrs. The standard solar model assumes that there is no mass loss or accretion during the evolution and hence the mass remains fixed. However, in general the radius and luminosity at current age will not match the observed values. In order to get the correct radius and luminosity, we adjust the mixing length parameter, α and the initial helium abundance Y_0. The initial heavy element abundance is adjusted to get the current value near the surface. Until recently, the helium abundance at the solar surface was not reliably determined and its value was estimated from the solar models. Now it is possible to estimate helium abundance using helioseismology and this value can be compared with that in a standard solar model to provide an independent test of solar models.

The resulting standard solar model has a central temperature of about 15.6×10^6 K and a density of about 150 g cm^{-3}, while at the surface the temperature drops to about 5800 K and density is 3×10^{-7} g cm^{-3}. The surface density is more than 1000 times lower than the density of Earth's atmosphere, while the pressure at solar surface is about 10^5 dynes cm^{-2}, which is about a tenth of that at the Earth's surface. The density and pressure decrease very rapidly with height in the solar atmosphere, while temperature initially decreases to about 4200 K, before rising rapidly in the corona. Although the temperature of the solar corona is very high, its density is very low and hence it doesn't need much energy to heat it up. A small fraction of the energy coming out from the Sun would be sufficient to maintain the corona at high temperatures, though we do not understand exactly how the energy gets deposited in this layer.

The total luminosity[11], $L_\odot = 3.842 \times 10^{33}$ erg s^{-1} is produced through nuclear reactions. The basic fusion reaction converts four protons to a helium nucleus, releasing about 26 MeV in the process along with two neutrinos. Of course, four protons are unlikely to interact simultaneously and the reaction actually takes place in a number of steps, known as the pp-cycle (e.g. Cox and Giuli[10]), which is responsible for most of the energy production in the Sun. From this, we can easily estimate that the Sun produces about 2×10^{38} neutrinos every second, giving a flux of about 7×10^{10} cm^{-2} s^{-1} at the Earth. It is these neutrinos which gave first direct evidence that nuclear reactions are responsible for production of solar energy.

Observations of solar oscillations

Fluid motions near the solar surface can be detected through Doppler shift in the spectral lines. Leighton *et al.*[12] found a quasi-periodic signal in the surface velocity with a period of approximately 5 min. This led to the discovery of the so-called five-minute oscillations. At that time, the nature of these oscillations was not clear and many theories were put forward to explain them. Ulrich[13] and Leibacher and Stein[14] suggested that these oscillations represent the acoustic modes of oscillation of the

entire Sun, which are trapped in the layers just below the surface. They predicted that in this case, the power would be concentrated in well-defined ridges in the k–ω diagram, where k is the spatial wave-number and ω the temporal frequency. Observations by Deubner[15] confirmed this prediction, thus establishing the nature of solar oscillations. Once the nature of these oscillations was established, it became clear that these can be used to study the solar interior, as the frequencies of these oscillations would be determined by the solar structure and dynamics. Initial observations of solar oscillations had limited spatial and temporal resolution and hence it was not possible to identify individual modes of solar oscillations. Subsequently, a number of attempts were made to detect oscillations over a wide range of length and time-scales. Helioseismic observations can be divided into two broad classes, one where the signal is averaged over the solar disk and another where a spatially resolved image of the Sun is used. The former is sensitive only to modes with length scale comparable to the solar radius. In the latter case depending on the resolution of the image used, we can observe modes with lower length scale. One of the first extensive tables of oscillation frequencies was provided by Libbrecht *et al.*[16] from observations made from the Big Bear Solar Observatory during 1986–1990. This table was extensively used in early helioseismic studies.

In order to determine the frequencies accurately and to resolve peaks with close frequencies, we need long observations. From most sites on Earth, the Sun can be observed continuously for a period of order of 12 h only. Periodic interruptions in observations caused by the day-night cycle lead to side lobes in the power spectra, which can interfere with other peaks. Thus, it is necessary to get continuous observations over a longer period of time. The first attempt was made by observing from a site near the geographic south pole[17]. Although in principle, we can observe the Sun continuously for 6 months from the south pole, in practice, because of weather conditions, it is difficult to get continuous observations over periods longer than 15 days. Another alternative is to observe from a network of sites around the Earth. The first network to be operational was the Birmingham Solar Oscillations Network (BiSON) which observes the oscillations in integrated light[18] and hence is sensitive only to large length scale modes. The main source of ground-based seismic data is the Global Oscillation Network Group (GONG) which has a network of six sites around the world[19] and currently images the Sun on a 1024×1024 CCD. This network became operational in May 1995 and is continuing observations so far with duty cycle approaching 90%. Apart from GONG, the other main source of helioseismic data is the Michelson Doppler Imager (MDI) instrument[20] on board the Solar and Heliospheric Observatory (SOHO) satellite which is located at the Lagrangian point between the Sun and the Earth, and hence gets an uninterrupted view of the Sun. SOHO was launched in December 1995 and regular observations have been going on since May 1996, except for a gap around 1998, when contact with the satellite was lost. The GONG and MDI instruments are currently the main sources of helioseismic data. The MDI instrument is planned to be superseded by the Helioseismic and Magnetic Imager (HMI) on the Solar Dynamics Observatory (SDO), which is expected to be launched in 2009.

Since the Sun is spherically symmetric to a good approximation, the modes of solar oscillations can be expressed in terms of spherical harmonics, $Y_{\ell m}(\theta, \phi)$, which determines the surface variation associated with the modes. The degree ℓ determines the length scale of the mode. The spatially resolved observations measure the line-of-sight velocity, v_s at each point on the solar surface as a function of time. This velocity is decomposed in terms of the spherical harmonics

$$v_s(\theta, \phi, t) = \sum_{\ell m} A_{\ell m}(t) Y_{\ell m}(\theta, \phi). \quad (5)$$

The amplitude of each component, $A_{\ell m}$, should include contributions from all modes with same values of ℓ and m. The Fourier transform of $A_{\ell m}(t)$ then gives the frequencies of all these modes. In practice, the decomposition in eq. (5) is not perfect, because we can observe less than half of the solar surface and that too with some projection which combines contribution from radial and tangential components of the velocity. As a result, the spherical harmonics are not orthogonal over the limited surface and each component has some leakage from the neighbouring modes. This leakage has to be accounted for while identifying peaks due to different modes in the power spectra. The maximum value of ℓ that can be studied depends on the resolution of image, while the maximum frequency that can be studied depends on the temporal resolution of observations. Most helioseismic observations are taken at a cadence of 1 per minute, which gives a Nyquist frequency of 8.333 mHz and only frequencies below this can be observed. The frequency resolution in the power spectra depends on the duration of the observations. For observations over one full-day the resolution is $1/86400 \approx 11.6$ μHz, which is not sufficient to resolve close peaks. The GONG project uses a time-series of 108 days giving a frequency resolution of 0.107 μHz. However, the ability to resolve close peaks in the power spectra also depends on the intrinsic width of the peaks, which is determined by the lifetime of the modes. The lifetime of modes decreases with increasing frequency and ℓ. Thus, modes with high frequency or degree are difficult to separate. As a result, modes with frequency larger than 3.5 mHz are not particularly reliable. The GONG frequency tables give frequencies of modes with $\ell \leq 150$, while MDI tables have some modes with higher ℓ, with the fundamental or f-modes going up to $\ell = 300$.

The modes of solar oscillations are characterized by three quantum numbers, n, ℓ, m, where n is the radial order, which is some measure of the number of nodes in the radial direction, while the degree ℓ and the azimuthal order m determines the variation with latitude and longitude. In the absence of rotation and magnetic field, the Sun would be spherically symmetric and the frequencies $\nu_{n\ell m}$ would be independent of m. Rotation and magnetic field lifts this degeneracy, giving rise to splitting of modes, which are measured by the splitting coefficients, defined by

$$\nu_{n\ell m} = \nu_{n\ell} + \sum_{j=1}^{J_{\max}} c_j^{n\ell} \mathcal{P}_j^{\ell}(m), \tag{6}$$

where $\nu_{n\ell}$ is the mean frequency of the multiplet, $c_j^{n\ell}$ the splitting coefficients and $\mathcal{P}_j^{\ell}(m)$ are orthogonal polynomials of degree j in m. Here the number of splitting coefficients determined, $J_{\max}$ is much less than $2\ell + 1$ and hence can be determined to higher accuracy. The mean frequency $\nu_{n\ell}$ is determined by the spherically symmetric structure of the Sun, while the splitting coefficients are determined by rotation, magnetic field and any other departures from spherical symmetry. It turns out that to first-order rotation gives rise to only odd terms in m giving the odd order splitting coefficients. The even order splitting coefficients can arise from second-order effect of rotation, magnetic field or other departures from spherical symmetry. Thus, although the effect of rotation can be separated from other sources, it is not possible to distinguish between the effect of magnetic field and other asphericities in the solar structure. Again to first order, only the north–south symmetric component of rotation rate contributes to the splittings, and thus the splitting coefficients contain little information about the north–south antisymmetric component of rotation rate. Similarly, the meridional flows can only contribute to the even order splitting coefficients and their effect is rather small. Both meridional flows and the north–south antisymmetric component of rotation can be studied using local helioseismic techniques (e.g. Gizon and Birch[21]) in the near surface region.

Theory of solar oscillations

The natural frequencies of a solar model can be easily determined by considering a small perturbation from the equilibrium model. For simplicity, the perturbations are assumed to be adiabatic, i.e. there is no exchange of energy between the perturbed elements and the surroundings. This assumption is valid in most of the solar interior where the time-scale for thermal energy exchange is much larger than the oscillation period of a few minutes. Unfortunately, this assumption breaks down near the surface where the thermal time-scale is of order of a few minutes and hence non-adiabatic effects can be important. The main reason for neglecting non-adiabatic effects is that there is no formulation to treat the perturbation in convective flux, although some attempts have been made to generalize the mixing length theory to time-dependent situations (e.g. Balmforth[22]). Apart from this the treatment of perturbation to radiative flux can also get complicated in the optically thin regions of the atmosphere (e.g. Christensen-Dalsgaard and Frandsen[23]). As a result, conventionally the frequencies of a solar model are computed by solving the adiabatic oscillation equations (e.g. Christensen-Dalsgaard[24]). Since non-adiabatic processes are important only near the surface, their effect can be eliminated by using other properties of solar oscillations. Further, since the amplitude of individual oscillation mode is rather small, the perturbations are treated in linear approximation giving rise to an eigenvalue problem for the linear adiabatic oscillation equation. The discrete eigenvalues of these equations define the frequency of individual modes.

The properties of solar oscillations are determined by the two critical frequencies, namely, the Lamb frequency, S_ℓ and the Brunt Väisälä a frequency, N,

$$S_\ell^2 = \frac{\ell(\ell+1)c^2}{r^2}, \tag{7}$$

$$N^2 = g_0 \left(\frac{1}{\Gamma_1} \frac{\mathrm{d}\ln p_0}{\mathrm{d}r} - \frac{\mathrm{d}\ln \rho_0}{\mathrm{d}r} \right), \tag{8}$$

where c is the speed of sound, r the radial distance, g_0 the acceleration due to gravity, Γ_1 the adiabatic index, ρ_0 the density and p_0 the pressure in equilibrium solar model. The Brunt Väisälä frequency is essentially the frequency of oscillation of a small element of fluid under buoyancy when it is displaced from its equilibrium position. If $N^2 > 0$ the fluid element is stable to perturbation and will oscillate about its equilibrium position with frequency N. On the other hand, if $N^2 < 0$, the fluid is unstable and a perturbation will lead to convection. This is essentially the criterion to determine onset of convection and for a uniform composition it reduces to the well-known Schwarzschild's criterion. Figure 1 shows these critical frequencies in the solar interior. Analysis of the equations of adiabatic oscillations suggests that there are two main types of oscillatory modes, the acoustic modes which are essentially sound waves where the pressure gradient provides the main restoring force, and the gravity modes where the restoring force is mainly provided by buoyancy. These gravity waves should not be confused with gravitational waves, which arise in the general theory of relativity. Although the gravity modes can in principle, yield gravitational waves from the Sun[25,26] which may be detectable by the proposed Laser Interferometer Space Antenna (LISA).

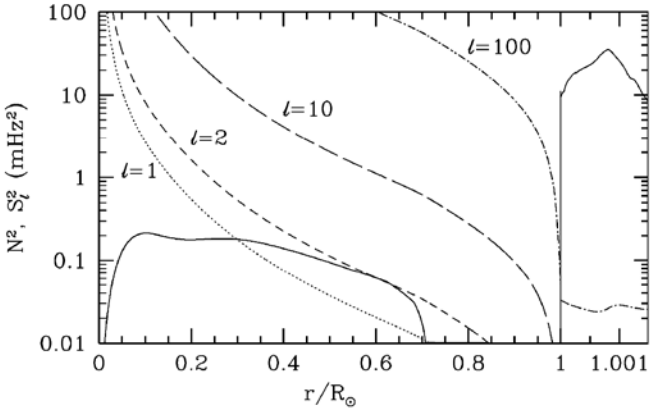

Figure 1. The frequencies N^2 and S_ℓ^2 in a standard solar model. The continuous line is N^2, while other lines show S_ℓ^2 for different values of ℓ as marked in the figure.

If the frequency $\omega_{n\ell m} > \max(S_\ell, N)$, then the oscillation behaves like an acoustic wave, while if $\omega_{n\ell m} < \min(S_\ell, N)$ we get gravity wave. For the intermediate values of frequency, the modes are evanescent, that is, the eigenfunction falls of exponentially with distance. Thus, the acoustic modes are trapped in regions where the frequency is larger than both S_ℓ, N. In the convection zone, $N^2 < 0$ and we cannot have gravity modes. Similarly, for $\ell = 0$ or the radial modes, $S_\ell = 0$, again it is not possible to get gravity modes. This can be understood from the fact that for $\ell = 0$, the entire surface would move up or down together as there is no dependence on θ, ϕ, while buoyancy can be effective only if there is some density difference at the same r. Thus, for radial modes the buoyancy is ineffective and we cannot get gravity modes.

In the solar interior the sound speed varies from about 7 km s^{-1} at the surface to about 500 km s^{-1} near the centre. Thus, the frequency S_ℓ increases sharply with depth and tends to infinity at the centre. S_ℓ also depends on ℓ, being essentially proportional to ℓ_i, for large ℓ. The frequency $N^2 < 0$, in the convection zone and also tends to zero at the centre. In the radiative interior it has a broad peak with a value of about 0.5 mHz. The maximum value of N in radiative interior defines the maximum frequency of internal gravity modes. Above the convection zone, the value of N increases very rapidly to about 5 mHz and is of the same order in lower atmosphere. In this region, S_ℓ is very small and thus the value of N in the atmosphere essentially determines the maximum frequency of acoustic modes that are trapped below the solar surface. Acoustic modes with larger frequency would be propagating in the atmosphere and their frequencies cannot be calculated reliably, as they will depend on where exactly the boundary condition is applied. On the other hand, if the modes are trapped in the interior, the eigenfunctions are falling off exponentially with height and the exact location of the boundary is not very crucial in determining the frequency. Thus, we generally use only modes trapped in the interior for helioseismic studies. If the modes are propagating in the atmosphere, the energy will leak out and such modes have small lifetime.

The classification into acoustic (also denoted as p-modes) and gravity (or g-modes) modes may not be unambiguous. Depending on the frequency, in some cases the same mode may behave like a gravity mode in the interior and an acoustic mode in the outer convection zone. Although, there are ways of classifying the modes into two series, for the Sun the ambiguity arises only for low frequency and low degree modes, which have not been observed so far. By convention, positive values of n denote p-modes and negative values denote g-modes, while $n = 0$ is referred to as fundamental or f-mode. At high degree, the f-mode is essentially a surface gravity mode with frequency given by $\omega^2 \approx g\sqrt{\ell(\ell+1)}/r$. Hence these modes have been used to measure solar radius as mentioned earlier. The observed solar oscillations have frequencies above approximately 0.9 mHz and hence these cannot be internal gravity modes. The p-modes with frequency less than about 5 mHz are trapped below the solar surface. The lower boundary of the trapping region is determined by the layer where $\omega = S_\ell$. This can also be understood in terms of sound waves travelling in a medium where sound speed increases with depth, due to increase in temperature. If we consider a sound wave travelling inwards from the surface, then it tends to deviate away from the radial direction because of refraction until it reaches a layer where it suffers total internal reflection and is reflected back to the surface. It can be seen that the point where it gets reflected is given by $\omega = S_\ell$. Thus, low degree modes can penetrate deep into the interior, while high degree modes are trapped in a shallow layer just below the surface. Similarly, in latitudinal direction the region where a mode is concentrated is determined by the value of m/ℓ. For $m = \pm \ell$ the mode is concentrated near the equator and as $|m/\ell|$ reduces it extends more to higher latitudes. Because of this property, each mode is trapped in a different region of the solar interior and its frequency is determined by structure of that region. As a result, by involving a large set of modes we can study different regions of the solar interior.

There is fairly good agreement between the observed frequencies and those computed for a solar model and it shows that the solar model is a good representation of the Sun. Nevertheless, the differences are much larger than the error-bars in observed frequencies and hence in that sense there is a significant difference between a model and the Sun. In order to study the solar interior, there are two possibilities, referred to as the forward or inverse techniques. In the forward approach, we can construct solar models with different input physics and compare their frequencies with observed frequencies to find out which model gives the best agreement (e.g. Elsworth *et al.*[27]). Most of the early inferences were obtained using the forward technique. For example, solar models with

low neutrino fluxes were ruled out in this manner. It was soon realized that the depth of the convection zone in the then prevalent solar models was on lower side[28] and needed to be increased to a value close to 200 Mm. Similarly, it was found that the treatment of convective flux, due to Canuto and Mazzitelli[29] led to better agreement as compared to the usual mixing length theory[30]. However, it was soon realized that the forward approach has severe limitations as no solar model is in perfect agreement with observations and moreover there is strong correlation between different effects, thus making it difficult to isolate the effect of one parameter in solar model. As a result, inverse techniques were developed, where we attempt to infer the internal structure directly from the observed frequencies.

In principle, the inverse technique can directly provide the structure variables like sound, speed and density in the solar interior without involving a solar model. In practice, most useful inversion methods are differential in nature giving a small correction to a reference solar model in terms of the observed frequency differences. Further, the inverse problems are necessarily ill-conditioned as we are attempting to determine a continuous function using only a finite set of modes. This problem is handled by restricting the structure function like the sound speed to a class of smooth functions. Various inversion techniques differ in the manner in which smoothness is enforced. The smallest length scale on which the variation can be reliably determined is referred to as the resolution of inverse technique and also depends on the number of modes that are available and the estimated error-bars in the observed frequencies. The resolution also depends on the depth as the number of modes that penetrate to a given depth reduces with increasing depth.

Inversion for solar structure is based on variational formulation of the eigenvalue problem for adiabatic oscillations equation[31] which gives an equation of the form

$$\frac{\delta\nu_{n\ell}}{\nu_{n\ell}} = \int_0^R K^{n\ell}_{c^2,\rho}(r)\frac{\delta c^2}{c^2}(r)\mathrm{d}r + \int_0^R K^{n\ell}_{\rho,c^2}(r)\frac{\delta\rho}{\rho}(r)\mathrm{d}r + \frac{F(\nu_{n\ell})}{E_{n\ell}}, \quad (9)$$

where the kernels $K^{n\ell}_{c^2,\rho}(r)$ and $K^{n\ell}_{\rho,c^2}(r)$ are determined by the eigenfunctions in the reference model (e.g. Antia and Basu[32]). The perturbations $\delta\nu_{n\ell}$, δc^2 and $\delta\rho$ can represent the difference between the Sun and a solar model (or between two solar models) and $E_{n\ell}$ is the mode inertia defined by

$$E_{n\ell} = \frac{4\pi\int_0^R [|\xi(r)|^2 + \ell(\ell+1)|\eta(r)|^2]\rho_0 r^2\mathrm{d}r}{M_\odot[|\xi(R_\odot)|^2 + \ell(\ell+1)|\eta(R_\odot)|^2]}, \quad (10)$$

where ξ and η are the radial and horizontal components of the displacement eigenfunction respectively. The last term in eq. (9) accounts for the uncertainties arising from outermost layers which are not resolved by the set of modes that may be available. This can also include the non-adiabatic effects which are not included in the equations for adiabatic oscillations. These equations can be solved, using various inversion techniques that have been developed (e.g. Gough and Thompson[33]). It turns out that most of the frequency differences between a solar model and the Sun are due to uncertainties in surface layers (e.g. Christensen-Dalsgaard *et al.*[34]).

Helioseismic study of solar structure

One of the important achievements of inversion technique is the inference of sound speed and density in the solar interior (e.g. Gough *et al.*[35], and Kosovichev *et al.*[36]). The sound speed in the bulk of the solar interior is known to an accuracy of better than 0.1%. From early inversion results, it became clear that there was some discrepancy in the sound speed in solar models just below the base of the convection zone. This was thought to be due to the then prevailing opacity tables and it was estimated that the opacities need to be increased by about 15–20%. This was soon confirmed by revised OPAL opacity calculations of Rogers and Iglesias[37]. After correcting for opacities, the remaining discrepancy was found to be due to neglect of diffusion of helium and heavy elements in the radiative interior[38]. After incorporating these improvements the standard solar model was found to be in very good agreement with solar structure inferred from inversion with maximum difference in sound speed of about 0.2% (ref. 34). Figure 2 shows the relative difference in sound speed between the Sun and some solar models. The inclusion of diffusion of helium in stellar evolution calculations affects other stars too and in particular it leads to depletion of hydrogen in the stellar core. As a result, the main sequence lifetime of stars is reduced when diffusion of helium in the radiative interior is included, which in turn reduces the estimated age of globular clusters[39]. This helps in resolving the age problem in cosmology, as the estimated ages of some globular clusters were found to be larger than the age of the Universe.

The main discrepancy in sound speed is found to be just below the base of the convection zone and it can be alleviated if a moderate amount of turbulent mixing, possibly due to rotationally induced instability, is included[40,41]. This region which is known as tachocline, has a high radial shear due to radial gradient in rotation rate, which may be responsible for the observed mixing. As seen from Figure 2, models with mixing in the tachocline region have better agreement with the Sun in the tachocline region. The discrepancy in the near surface region is most probably due to incorrect solar radius. This is difficult to address, as it is primarily due to errors in modelling the near surface regions, because of which the

position of the solar surface cannot be determined accurately in a solar model. The uncertainty in the position of surface being of an order of 100 km. Since the pressure and density scale heights at the solar surface are also about 100 km, this shift in surface by 100 km, can lead to significant errors when differences are taken at constant fractional radius between a solar model and the Sun.

The sound speed is given by $\sqrt{\Gamma_1 P/\rho}$ and is also affected by the adiabatic index Γ_1. Through most of the solar interior, the dominant constituents, hydrogen and helium are almost fully ionized. However, near the surface these elements are not ionized and most of the free electrons are contributed by metals with low ionization potential. In the regions where the gas is fully ionized (or fully unionized) the adiabatic index $\Gamma_1 = (\partial \ln P/\partial \ln \rho)_S \approx 5/3$, where the derivative is taken at constant entropy. In the ionization regions the value of Γ_1 dips below the ideal gas value of 5/3. The extent of dip is also determined by the composition of the solar material and hence can be used to determine the helium abundance in the solar convection zone. For this purpose, it is convenient to use the dimensionless gradient of squared sound speed

$$W(r) = \frac{1}{g}\frac{\mathrm{d}c^2}{\mathrm{d}r}. \tag{11}$$

In the lower part of the convection zone where the temperature gradient is close to the adiabatic value and the gas is mostly ionized, $W(r) \approx -2/3$. Below the convection zone $W(r)$ is determined by the temperature gradient and its value increases rapidly. There is a discontinuity in the first derivative of $W(r)$ at the base of the convection zone (see Figure 3). This was used to get an accurate measure of the position of the base of the convection zone[42], $r_b = (0.713 \pm 0.001)R_\odot$. The frequencies of solar oscillations are sensitive to the depth of the convection zone and hence this can be determined accurately from the observed frequencies. The position of the base of the convection zone in a solar model is determined by the opacities and this provides a test of opacities[43]. It was found that the OPAL opacity tables with the then heavy element abundances[44] were consistent with seismic data.

Apart from the depth of the convection zone, $W(r)$ can also be used to determine the composition of the solar convection zone. In the ionization zones of various elements, Γ_1 dips below the ideal value of 5/3 while $W(r)$ shows a peak. The height of the peak depends on abundance of the element undergoing ionization and can be calibrated to determine its abundance. In particular, it is not possible to determine abundance of helium and other noble gases from the photospheric spectrum as these elements do not form lines at relatively low temperatures in the photosphere. Although, coronal lines of these elements are known, it is difficult to get a reliable estimate of abundances from these because of lack of adequate models of coronal region. Currently, helioseismology provides the most reliable measure of helium abundance. In the HeII ionization zone located around $r = 0.98R_\odot$, the function $W(r)$ has a sharp peak which has been used to determine helium abundance (e.g. Basu and Antia[45]). Apart from abundance, the height and shape of the peak (or the dip in Γ_1) in a solar model also depends on the equation of state. Thus, it can also be used to test the equation of state[45,46]. It was found that the equations of

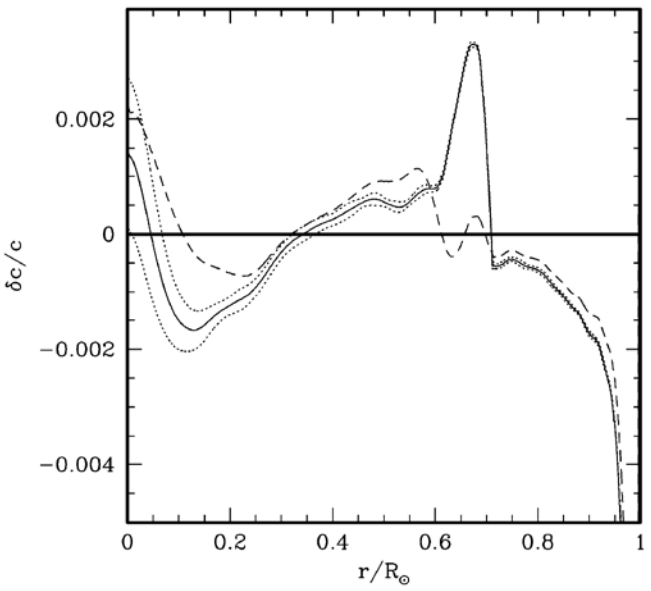

Figure 2. Relative difference in sound speed and density profiles between the Sun and the standard solar model of Christensen-Dalsgaard *et al.*[34] is shown by continuous lines. The dotted lines show 1σ error-bars. The dashed lines show the result for a model with mixing in the tachocline[53].

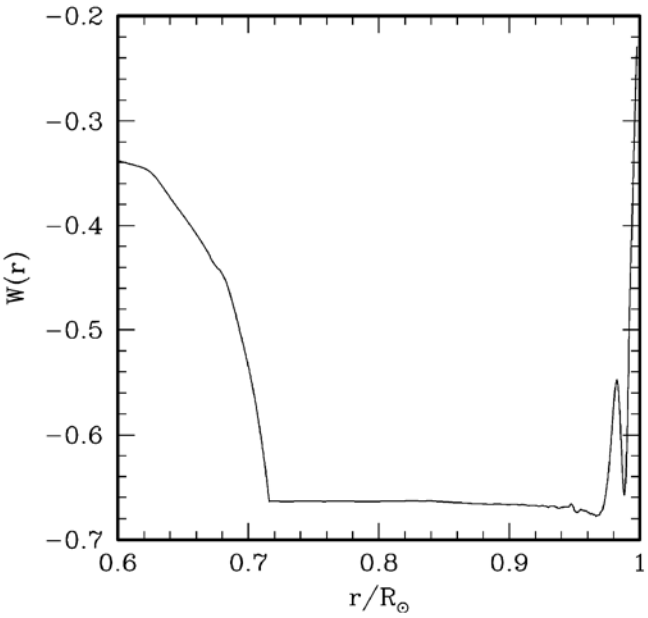

Figure 3. The function $W(r)$ for a solar model.

state used early on were not good enough to model the solar convection zone. In particular, the Coulomb corrections to the equation of state are important in this region[47]. More sophisticated equations of state like the Mihalas, Hummer and Döappen (MHD)[48] or OPAL[49] equations of state give better agreement with helioseismic data. Further, the OPAL equation of state is found to be in better agreement with solar data as compared to the MHD equation of state[45]. These equations of state were also found to be discrepant in the core due to neglect of relativistic corrections for electrons[50]. This discrepancy is now corrected in the later version of OPAL equation of state[51]. In principle, abundance of heavy elements can also be determined through similar procedure, but the main problem is due to the low abundance of heavy elements the height of resulting peak is very small and moreover ionization zones of various elements overlap with each other, thus making it difficult to separate out the contribution from individual elements.

The adiabatic oscillation equation depends only on sound speed and density and it is not possible to determine other structure variables, like temperature directly from seismic inversions. However, once sound speed and density are known, we can use the equations of thermal equilibrium (eqs (3) and (4)) to determine the temperature and composition in the radiative interior (e.g. Antia and Chitre[52]). Only one component of the composition can be determined and hence generally we use a known heavy element abundance profile to determine the helium abundance and temperature using these equations. These profiles are again found to be close to those in a standard solar model (e.g. Brun *et al.*[53]). The abundance profile just below the base of the convection zone is found to be flat, thus confirming the operation of mixing process inferred earlier. This mixing also explains the low observed lithium abundance at solar surface as compared to that in meteorites. Lithium can be destroyed by nuclear reactions at fairly low temperatures of about 2.5×10^6 K, but the temperature at the base of the convection zone is somewhat lower. Hence, if the mixing is confined to the convection zone, lithium cannot be destroyed. But, if the mixing extends to a layer further down, lithium can be destroyed, thus explaining the low abundance at the surface. Abundances of lithium and beryllium provide strong constraint on the extent of mixing below the convection zone as the temperature in the mixed region should be enough to destroy Li, but not high enough to destroy Be. Once these abundance and temperature profiles are determined, we can calculate the total energy generated in the solar core and the value can be compared with the known solar luminosity, thus giving a test of the heavy element abundance profile and other input physics like the nuclear energy generation rate[54]. It is possible to put limits on the heavy element abundance Z using these constraints.

While excellent agreement between standard solar model and seismically inferred profiles has been achieved when the heavy element abundances from Grevesse and Noels[44] were used. This abundance tables gives $Z/X = 0.0245$, which was revised to 0.023 by Grevesse and Sauval[55]. But this marginal revision did not have much effect on solar models. However, these abundances were drastically revised by Asplund *et al.*[56] who used improved 3D atmospheric models to compute abundances from spectroscopic data. The main effect was through reduction of oxygen and other abundant elements like C, N, Ne, to reduce Z/X to 0.0165. With reduced Z, the opacities reduce and the resulting solar model has significant discrepancy near the base of the convection zone. Since then, a considerable effort has been made to reconcile seismic data with reduced abundances and all attempts made so far have failed (cf. Basu and Antia[57]). In fact, models with low Z were already considered for solving the solar neutrino problem, and were ruled out from other considerations. Attempts have been made to determine Z using seismic techniques[58] based on $W(r)$, and this gives $Z = 0.017 \pm 0.002$, which is consistent with old abundances. Thus there is a serious discrepancy between seismic evidence and the revised heavy element abundances. With old abundances of Grevesse and Sauval[55] the solar models are in excellent agreement with seismic profiles, while with revised abundance it is not possible to restore this agreement, unless all physical inputs, like opacities, equation of state, diffusion rates are modified beyond their normally accepted uncertainties. It is clear that more effort is needed to confirm the revised abundances through independent 3D atmospheric models and other techniques. Recent work in this direction is pointing to increased abundances[59,60] of oxygen. It is clear that there is some uncertainty in abundances and we need to explore all techniques to determine these abundances.

Rotation rate in the solar interior

Solar surface rotation has been extensively studied through observations of tracers like sunspots or other magnetic features or through Doppler measurements[61]. It is well-known that the Sun does not rotate like a rigid body, but has differential rotation, with equator rotating faster than the poles. Further, observations of young stars suggest that they are rotating much faster and hence it is believed that the Sun has lost considerable angular momentum through the solar wind. The exact theory of angular momentum transport in the Sun is not sufficiently developed to predict the current profile of solar rotation. It was generally thought that the solar core would be rotating faster than the surface and this would have consequences for the test of general relativity using the observed precession of the orbit of planet Mercury[62,63]. If the solar core is rotating fast enough, it would distort the Sun producing a quadrupole moment, which is turn would contribute to the precession of orbit through purely

Newtonian effects, thus introducing a discrepancy between the observed precession and the value predicted by general relativity. Thus, there was considerable interest in determining the rotation profile in the solar interior. This became possible with advent of helioseismology, as the rotational splitting of modes, depends on internal rotation and by measuring the splittings of a large set of modes, it is in principle, possible to infer the rotation rate in the interior.

Rotation rate in the solar interior is normally inferred through inversion of equations connecting the rotational splittings to the rotation rate. This equation can be derived by treating rotation terms as small perturbation to the variational formulation of the equation of adiabatic oscillations and can be formally written as

$$c_j^{n\ell} = \int_0^1 \int_0^1 \mathrm{d}r \, \mathrm{d}\cos\theta \, K_{n\ell j}(r, \theta)\Omega(r, \theta), \tag{12}$$

where Ω is the rotation rate, θ the colatitude and $K_{n\ell j}$ are the kernels which depend on the eigenfunctions in the spherically symmetric model (e.g. Pijpers[64]). These equations can be inverted to obtain the rotation rate as a function of r, θ from the observed splittings. Only odd coefficients are needed for this purpose, as the integrals vanish for the even coefficients.

Early inversions for the rotation rate[65,66] showed that the differential rotation persists through the convection zone, but below the convection zone, there is a sharp transition to nearly rigid-body rotation rate. This picture has now been confirmed by better data from GONG and MDI[67,68]. Figure 4 shows the temporally averaged rotation rate inferred from MDI data. The transition region near the base of the convection zone is called the tachocline[69] and is believed to be the region where the solar dynamo operates. The rotation rate in the radiative interior is found to be comparable to the surface value around the latitude of 30°. Although, it is difficult to determine the rotation rate in the core, because of lack of reliable splittings for low degree modes, the estimated errors are not expected to be particularly large. These certainly rules out significantly faster rotation in the solar core and consequently large quadrupole moment[70]. Thus helioseismic inversions for rotation rate support general relativity. Apart from the tachocline, there is another shear layer just below the solar surface where the rotation rate increases with depth. This shear layers extends to a depth of about $0.05R_\odot$.

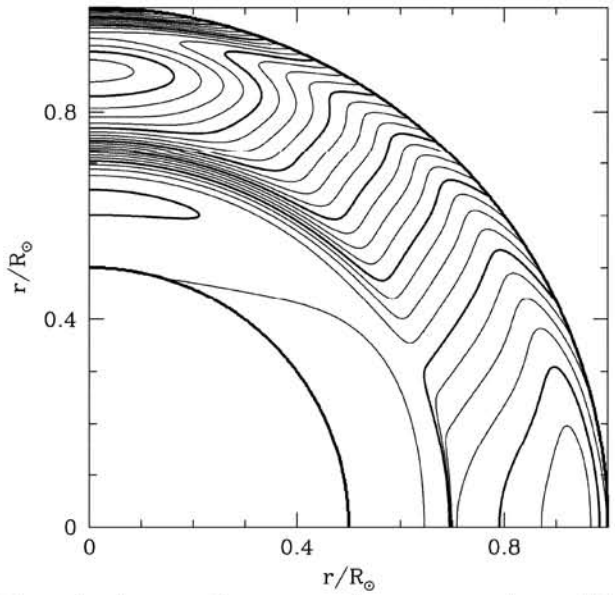

Figure 4. Contours of constant rotation rate averaged over all MDI data as obtained by 2*d* inversion technique. Due to the symmetry of the inversion results, the rotation rate has been shown for just one quadrant only. The light contours have been drawn at intervals of 5 nHz, while the heavy lines are at intervals of 20 nHz. The *x*-axis represents the solar equator while the *y*-axis represents the rotation axis.

The inferred rotation rate in the solar interior is found to be quite different from what was predicted by theoretical calculations[71,72], which showed that rotation rate should be constant on cylinders aligned with the rotation axis. Recent numerical simulations appear to be able to get a profile close to that inferred from helioseismology. However, the origin of tachocline is still not clear.

With the availability of helioseismic data over the last solar cycle 23, it is possible to study temporal variations in the solar structure and rotation over the solar cycle. Even early observations during solar cycle 22 established temporal variations in the solar oscillations frequencies[73,74]. The frequencies were found to increase with solar activity by up to 0.4 μHz. With the availability of better quality data from GONG and MDI, it was possible to study the temporal variations more reliably and it was quickly established that the frequency shift is well correlated with the solar activity indices[75] as seen in Figure 5. There was a strong frequency dependence in the frequency shift with shift increasing with increasing frequency. Further, it was found that frequency shift scaled

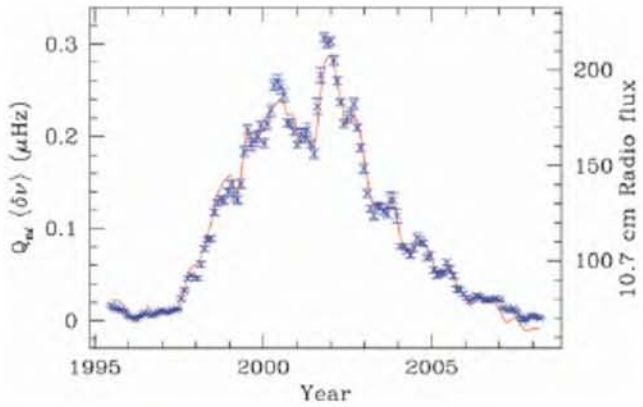

Figure 5. Mean frequency shift of p-modes as a function of time using GONG data is shown by the continuous line. The points with error-bars show the mean 10.7 cm radio flux on a scale marked on right-hand axis.

by mode inertia is only a function of frequency being largely independent of the degree ℓ. This suggests that the frequency shifts are largely a surface phenomenon and if the frequency differences are inverted to find corresponding structural changes, the variation would be confined near the solar surface. This temporal variation may be due to magnetic field near the solar surface, which is known to vary with solar cycle.

Apart from frequencies the splitting coefficients were also found to vary with solar cycle and these can be inverted to determine the rotation rate as a function of time. To find the temporally varying component of the rotation rate, it is convenient to subtract out the temporally averaged rotation rate at each radius and latitude to get the residual

$$\delta\Omega(r, \theta, t) = \Omega(r, \theta, t) - \langle\Omega(r, \theta, t)\rangle, \quad (13)$$

where the angular brackets denote temporal average. The residual $\delta\Omega$ defines the temporally varying part of the rotation rate. It is more convenient to define the associated velocity $\delta v_\phi = \delta\Omega r \sin\theta$, which is referred to as zonal flow velocity. The surface observations of solar rotation had already established a pattern of temporal variation with bands of faster (or slower) than average rotation moving towards the equator with time[76] referred to as torsional oscillations. Similar pattern was seen to persist in the solar interior[77,78]. The zonal flow velocity is of order of 10 m s^{-1}, which is about 0.5% of the rotation velocity. Thus, the variation in rotation rate is fairly small and high quality data was required to identify the pattern. With accumulation of more data from GONG and MDI it became clear that at high-latitudes the bands move towards the poles, with the transition happening around a latitude[79] of 45°. Figure 6 shows the results at $r = 0.98R_\odot$. These bands also move upwards with time at low latitudes with a speed of 1 ms^{-1}. Further, the pattern is found to penetrate to the base of the convection zone[80,81]. Thus as opposed to structure variation which appear to be confined to near surface regions, the variation in rotation rate penetrates deep inside the convection zone. More recent results covering almost complete solar cycle 23 are described by Howe *et al.*[87] and Antia *et al.*[82].

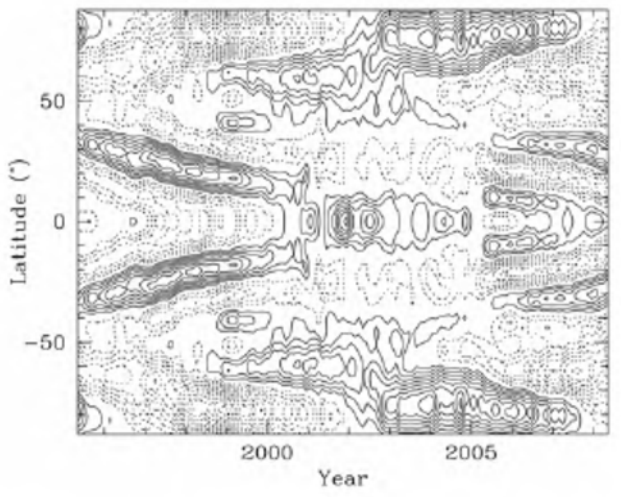

Figure 6. The contours of time varying component of rotation velocity, v_ϕ at a depth of 0.02 $R_\odot$ below the solar surface are shown as a function of latitude and time. The continuous contours are for positive δv_ϕ while dotted contours denote negative values. The contours are drawn at interval of 1 ms^{-1}.

Since the solar dynamo is believed to operate in the tachocline region, there is considerable interest in detecting temporal variations in this region. However, errors in inversions increase with depth and the magnitude of zonal flow velocity appears to reduce with depth, thus making it difficult to draw definite conclusions about temporal variations in the tachocline regions. Howe *et al.*[84] found a periodic variation at equatorial region around $r = 0.72R_\odot$ with a period of 1.3 years. However, other studies using the same data (e.g. Basu and Antia[81]) did not find this signal. Subsequently, Howe *et al.*[85] also did not find the oscillatory behaviour beyond 2001 and they have conjectured that this periodicity is seen only during the rising phase of a solar cycle. Further, observations during the next few years should be able to verify this.

Since differential rotation plays a central role in the dynamo, the zonal flow is believed to be a back reaction of the dynamo process on rotation and the zonal flow pattern can be computed from a dynamo model. This pattern can be compared with the observed pattern during the last solar cycle. There is a qualitative agreement between the two patterns (e.g. Covas *et al.*[86]), though the two patterns do not match in details. The observed zonal flow pattern provides a strong constraint on dynamo models and can be used to test these models. The dynamo action is determined by the gradients of the rotation velocity and these can be computed from the inverted profiles[83]. It turns out that the temporal variation in the gradients of rotation rate can be a significant fraction of its average value. Thus these variations would also play a role in dynamo models.

Continued seismic observations over the next solar cycle will improve our understanding of solar interior and would help us in understanding the solar dynamo and angular momentum transfer in solar interior.

This work utilizes data obtained by the GONG project, managed by the National Solar Observatory, which is operated by AURA, Inc. under a cooperative agreement with the National Science Foundation. The data were acquired by instruments operated by the Big Bear Solar Observatory, High Altitude Observatory, Learmonth Solar Observatory, Udaipur Solar Observatory, Instituto de Astrofisico de Canarias, and Cerro Tololo Inter-American Observatory. This work also utilizes data from the Solar Oscillations Investigation/Michelson Doppler Imager (SOI/MDI) on the SOHO. SOHO is a project of international cooperation between ESA and NASA. MDI is supported by NASA grants NAG5-8878 and NAG5-10483 to Stanford University.

1. Hale, G. E., *ApJ*, 1908, **28**, 315.
2. Davis, R., *PRL*, 1964, **12**, 303.
3. Goldreich, P. and Keeley, D. A., *ApJ*, 1977, **212**, 243.
4. Ahmad, Q. R. *et al.*, *PRL*, 2002, **89**, 011301.
5. Auwers, A., *AN*, 1891, **128**, 361.
6. Brown, T. M. and Christensen-Dalsgaard, J., *ApJ*, 1998, **500**, L195.
7. Schou, J., Kosovichev, A. G., Goode, P. R. and Dziembowski, W. A., *ApJ*, 1997, **489**, L197.
8. Antia, H. M., *A&A*, 1998, **330**, 336.
9. Christensen-Dalsgaard, J., Di Mauro, M. P., Schlattl, H. and Weiss, A., *MNRAS*, 2005, **356**, 587.
10. Cox, J. P. and Giuli, R. T., *Principles of Stellar Structure*, Gordon & Breach, New York, 1968.
11. Fröhlich, C. and Lean, J., *Geophys. Res. Lett.*, 1998, **25**, 4377.
12. Leighton, R. B., Noyes, R. W. and Simon, G. W., *ApJ*, 1962, **135**, 474.
13. Ulrich, R. K., *ApJ*, 1970, **162**, 993.
14. Leibacher, J. and Stein, R. F., *Astrophys. Lett.*, 1971, **7**, 191.
15. Deubner, F.-L., *A&A*, 1975, **44**, 371.
16. Libbrecht, K. G., Woodard, M. F. and Kaufman, J. M., *ApJS*, 1990, **74**, 1129.
17. Grec, G., Fossat, E. and Pomerantz, M., *Nature*, 1980, **288**, 541.
18. Chaplin, W. J. *et al.*, *Solar Phys.*, 1996, **168**, 1.
19. Harvey, J. W. *et al.*, *Science*, 1996, **272**, 1284.
20. Scherrer, P. H. *et al.*, *Solar Phys.*, 1995, **162**, 129.
21. Gizon, L. and Birch, A. C., *Liv. Rev. Sol. Phys.*, 2005, **2**, 6.
22. Balmforth, N. J., *MNRAS*, 1992, **255**, 632.
23. Christensen-Dalsgaard, J. and Frandsen, S., *Solar Phys.*, 1983, **82**, 165.
24. Christensen-Dalsgaard, J., *Rev. Mod. Phys.*, 2002, **74**, 1073.
25. Cutler, C. and Lindblom, L., *PRD*, 1996, **54**, 1287.
26. Polnarev, A. G., Roxburgh, I. W. and Baskaran, D., *Phys. Rev.*, 2009, **79**, 082001.
27. Elsworth, Y., Howe, R., Isaak, G. R., McLeod, C. P. and New, R., *Nature*, 1990, **347**, 536.
28. Gough, D. O., In *Energy Balance and Hydrodynamics of the Solar Chromosphere and Corona* (eds Bonnet, R. M. and Delache, P.), IAU Colloq. 36, G. de Bussac, Clermont-Ferrand, 1977, p. 3.
29. Canuto, V. M. and Mazzitelli, I., *ApJ*, 1991, **370**, 295.
30. Basu, S. and Antia, H. M., *J. Astrophys. Astron.*, 1994, **15**, 143.
31. Chandrasekhar, S., *ApJ*, 1964, **139**, 664.
32. Antia, H. M. and Basu, S., *A&AS*, 1994, **107**, 421.
33. Gough, D. O. and Thompson, M. J., In *Solar Interior and Atmosphere* (eds Cox, A. N., Livingston, W. C. and Matthews, M.), Space Science Series, University of Arizona Press, 1991, p. 519.
34. Christensen-Dalsgaard, J. *et al.*, *Science*, 1996, **272**, 1286.
35. Gough, D. O. *et al.*, *Science*, 1996, **272**, 1296.
36. Kosovichev, A. G. *et al.*, *Sol. Phys.*, 1997, **170**, 43.
37. Rogers, F. J. and Iglesias, C. A., *ApJS*, 1992, **79**, 507.
38. Christensen-Dalsgaard, J., Proffitt, C. R. and Thompson, M. J., *ApJ*, 1993, **403**, L75.
39. Chaboyer, B., Deliyannis, C. P., Demarque, P., Pinsonneault, M. H. and Sarajedini, A., *ApJ*, 1992, **388**, 372.
40. Richard, O., Vauclair, S., Charbonnel, C. and Dziembowski, W. A., *A&A*, 1996, **312**, 1000.
41. Brun, A. S., Turck-Chièze, S. and Zahn, J. P., *ApJ*, 1999, **525**, 1032.
42. Christensen-Dalsgaard, J., Gough, D. O. and Thompson, M. J., *ApJ*, 1991, **378**, 413.
43. Basu, S. and Antia, H. M., *MNRAS*, 1997, **287**, 189.
44. Grevesse, N. and Noels, A., In *Origin and Evolution of the Elements* (eds Prantzos, N., Vangioni-Flam, E. and Cassè, M.), Cambridge University Press, 1993, p. 14.
45. Basu, S. and Antia, H. M., *MNRAS*, 1995, **276**, 1402.
46. Basu, S. and Christensen-Dalsgaard, J., *A&A*, 1997, **322**, L5.
47. Christensen-Dalsgaard, J. and Däppen, W., *A&A Rev.*, 1992, **4**, 267.
48. Däppen, W., Mihalas, D., Hummer, D. G. and Mihalas, B. W., *ApJ*, 1988, **332**, 261.
49. Rogers, F. J., Swenson, F. J. and Iglesias, C. A., *ApJ*, 1996, **456**, 902.
50. Elliott, J. R. and Kosovichev, A. G., *ApJ*, 1998, **500**, L199.
51. Rogers, F. J. and Nayfonov, A., *ApJ*, 2002, **576**, 1064.
52. Antia, H. M. and Chitre, S. M., *A&A*, 1998, **339**, 239.
53. Brun, A. S., Antia, H. M., Chitre, S. M. and Zahn, J.-P., *A&A*, 2002, **391**, 725.
54. Antia, H. M. and Chitre, S. M., *A&A*, 1999, **347**, 1000.
55. Grevesse, N. and Sauval, A. J., *Space Sci. Rev.*, 1998, **85**, 161.
56. Asplund, M., Grevesse, N. and Sauval, A. J., In *Cosmic Abundances as Records of Stellar Evolution and Nucleosynthesis* (eds Barnes, T. G. and Bash, F. N.), ASP Conference Series, 2005, vol. 336, p. 25.
57. Basu, S. and Antia, H. M., *Phys. Rep.*, 2008, **457**, 217.
58. Antia, H. M. and Basu, S., *ApJ*, 2006, **644**, 1292.
59. Centeno, R. and Socas-Navarro, H., *ApJ*, 2008, **682**, L61.
60. Caffau, E. *et al.*, *A&A*, 2008, **488**, 1031.
61. Howard, R., *ARA&A*, 1984, **22**, 131.
62. Dicke, R. H. and Goldenberg, H. M., *ApJS*, 1974, **27**, 131.
63. Dicke, R. H., Kuhn, J. R. and Libbrecht, K. G., *Nature*, 1985, **316**, 687.
64. Pijpers, F. P., *A&A*, 1997, **326**, 1235.
65. Brown, T. M. and Morrow, C. A., *ApJ*, 1987, **314**, L21.
66. Brown, T. M., Christensen-Dalsgaard, J., Dziembowski, W. A., Goode, P., Gough, D. O. and Morrow, C. A., *ApJ*, 1989, **343**, 526.
67. Thompson, M. J. *et al.*, *Science*, 1996, **272**, 1300.
68. Schou, J. *et al.*, *ApJ*, 1998, **505**, 390.
69. Spiegel, E. A. and Zahn, J.-P., *A&A*, 1992, **265**, 106.
70. Pijpers, F. P., *MNRAS*, 1998, **297**, L76.
71. Gilman, P. A. and Miller, J., *ApJS*, 1986, **61**, 585.
72. Glatzmaier, G. A., In *The Internal Solar Angular Velocity* (eds Durney, B. R. and Sofia, S.), Dordrecht, Reidel, 1987, p. 263.
73. Libbrecht, K. G. and Woodard, M. F., *Nature*, 1990, **345**, 779.
74. Elsworth, Y., Howe, R., Isaak, G. R., McLeod, C. P. and New, R., *Nature*, 1990, **345**, 322.
75. Bhatnagar, A., Jain, K. and Tripathy, S. C., *ApJ*, 1999, **521**, 885.
76. Howard, R. and LaBonte, B. J., *ApJ*, 1980, **239**, L33.
77. Howe, R. *et al.*, *ApJ*, 2000, **533**, L163.
78. Antia, H. M. and Basu, S., *ApJ*, 2000, **541**, 442.
79. Antia, H. M. and Basu, S., *ApJ*, 2001, **559**, L67.
80. Vorontsov, S. V., Christensen-Dalsgaard, J., Schou, J., Strakhov, V. N. and Thompson, M. J., *Science*, 2002, **296**, 101.
81. Basu, S. and Antia, H. M., *ApJ*, 2003, **585**, 553.
82. Howe, R. *et al.*, *ApJ*, 2006, **649**, 1155.
83. Antia, H. M., Basu, S. and Chitre, S. M., *ApJ*, 2008, **681**, 680.
84. Howe, R. *et al.*, *Science*, 2000, **287**, 2456.
85. Howe, R., Christensen-Dalsgaard, J., Hill, F., Komm, R. W., Schou, J., Thompson, M. J. and Toomre, J., *Adv. Space Res.*, 2007, **40**, 915.
86. Covas, E., Tavakol, R., Moss, D. and Tworkowski, A., *A&A*, 2000, **360**, L21.

Reanalysis of rDNA-ITS2 region sequences of *Anopheles* cf. *culicifacies* 'Bluchistan' revealed conspecificity to *A. dthali*

K. Raghavendra*, B. P. Niranjan Reddy, A. P. Dash and Aparup Das

National Institute of Malaria Research, 22 Shamnath Marg, New Delhi 110 054, India

***Anopheles* cf. *culicifacies* 'Bluchistan' was reported as a new variant of *A. culicifacies* species complex based on internal transcribed spacer 2 (ITS2) region by Djadid and Saifi in 2001 (GenBank accession number AF_402296) and was later stated to be phylogenetically close to *A. culicifacies* sp. A. Though comparison of ITS2 sequences of the members of *A. culicifacies* sp. complex with *A.* cf. *culicifacies* 'Bluchistan' revealed appreciable polymorphism to state the existence of new species, local alignment search and phylogenetic analysis results showed the conspecificity to *A. dthali*. In short, the present study gives a case report of misidentification of a species that highlighted the importance of initial morphotaxonomical identification before conducting the computational molecular phylogenetic studies. Such misidentification may sometimes lead to the suggestion of wrong vector control strategies for disease management.**

Keywords: *Anopheles culicifacies*, *Anopheles dthali*, misidentification, phylogeny, rDNA-ITS2.

ANOPHELES culicifacies sensu lato, is recognized as a complex of five sibling species provisionally designated as species A, B (ref. 1), C (ref. 2), D (ref. 3) on the basis of diagnostic inversion genotypes on polythene chromosome, and species E based on Y-chromosome mitotic karyotype variations and sporozoite positivity[4]. Recently, different DNA markers, viz. cytochrome oxidase I (COI)[5], cytochrome oxidase II (COII)[6], internal transcribed spacer 2 (ITS2)[7,8] and 28S D3 region[9] are reported to distinguish different members of the *A. culicifacies* species complex.

In 2001, Djadid and Saifi (http://www.ncbi.nlm.nih.gov/nuccore/16903461) reported the presence of an entirely new species of *A. culicifacies* identified from Zeineddini, Baluchistan province and named it as *A.* cf. *culicifacies* 'Bluchistan' based on variance in ITS2 region of ribosomal DNA with the available sequences of members of the *A. culicifacies* complex.

Thereafter, using ribosomal DNA (rDNA)-ITS2, randomly amplified polymorphic DNA (RAPD) and simple sequence repeat (SSR) primers, this new species was reported to be distributed in wide geographic regions of Iran; in Koutiji, near Kerman Province and in Baluchistan of southeastern province. This species was earlier designated as sp. X (refs 10 and 11). Moreover, the author also reported a close identity of the new species *A.* cf. *culicifacies* 'Bluchistan' to *A. culicifacies* sibling species A at the ITS2 DNA sequence region (GenBank accession number AF_402297)[10].

The *ITS2* marker gene was extensively used to differentiate the members of various anophelines and their sibling species[12–14]. Though molecular techniques hold some merits over morphotaxonomical methods for species identification, the importance of the latter cannot be overlooked. In Vietnam, misidentification of *A. minimus* as *A. varuna* led to the suggestion of wrong vector control methods[15]. Here, we present a case of morphological misidentification, which has led to the report of existence of a new variant of *A. culicifacies* species that was actually *A. dthali*. *A. dthali* is reported as malaria vector of secondary importance with wide distribution in southern parts of Iran including Baluchisthan[16] and it is worth mentioning here that *A.* cf. *culicifacies* 'Bluchistan' was reported to have been collected from this area[10].

Available 20 DNA sequences of ITS2 region of the members of *A. culicifacies* complex (of which, 8 sequences were of sp. B, 7-sp. A, 2-sp. E, 1-sp. C and 1-sp. D) were downloaded from GenBank (http://www.ncbi.nlm.nih.gov/). To substantiate the data further, more specimens of species B, C and D were sequenced. Field collected specimens of *A. culicifacies* from villages of Alwar District (76°38′E long. and 27°34′N lat.; Rajasthan, north-west India), Surat District (72°54′ long. and 21°10′ lat.; Gujarat, West India), were identified to sibling species B, C and D, following COII-PCR assay[6], and used for sequencing. DNA was isolated following the procedure described in Collins *et al.*[17]. The rDNA-ITS2 region was amplified using primers ITS2a (TGTGAACTGCAGGACACAT) and ITS2b (TATGCTTAAATTCAGGGGGT), and by following the PCR protocol described in Goswami *et al.*[7]. The PCR product was cleaned using QIAquick PCR purification kit (QIAGEN) according to manufacturer's instructions. Direct sequencing was performed, transposing the cloning intermediate step, using the Big Dye® terminator v3.1 Cycle Sequencing Kit (Applied Biosystems) in volume of 10 µl containing 10 ηg of purified DNA and 2 µl of Big Dye terminator master mix, and 1.6 p moles of primer, according to manufacturer's instructions. Sequencing reactions were performed 25 cycles of 30 S at 96°C, 30 S at 50°C, 4 min at 60°C. Excess of dye terminators were removed by ethanol/sodium acetate precipitation method. Sequencing reactions were electrophoresed using the POP-4™ polymer on ABI PRISM® 3730 Genetic Analyser (Applied Biosystems).

The accession numbers of the new sequences were highlighted with asterisk mark (*) in Figure 1. Pairwise and multiple sequence alignments were performed using the program clustalX, version 1.83 (http://www-igbmc.u-strasbg.fr/BioInfo/ClustalX/)[18]. Inter- and intraspecific

*For correspondence. (e-mail: kamarajur2000@yahoo.com)